pp 415–434. © Royal Aeronautical Society 2016
doi: 10.1017/aer.2016.15

Structured non-self approach for aircraft failure identification within a fault tolerance architecture

H. Moncayo
moncayoh@erau.edu

I. Moguel
Department of Aerospace Engineering
Embry-Riddle Aeronautical University
Daytona Beach, Florida
US

M.G. Perhinschi
Department of Mechanical and Aerospace Engineering
West Virginia University
Morgantown, West Virginia
US

A. Perez
Department of Aerospace Engineering
Embry-Riddle Aeronautical University
Daytona Beach, Florida
US

D.Al Azzawi and A. Togayev
Department of Mechanical and Aerospace Engineering
West Virginia University
Morgantown, West Virginia
US

ABSTRACT

Within an immunity-based architecture for aircraft fault detection, identification and evaluation, a structured, non-self approach has been designed and implemented to classify and quantify the type and severity of different aircraft actuators, sensors, structural components and engine failures. The methodology relies on a hierarchical multi-self strategy with heuristic selection of sub-selves and formulation of a mapping logic algorithm, in which specific detectors of specific selves are mapped against failures based on their capability to selectively capture the dynamic fingerprint of abnormal conditions in all their aspects. Immune negative and positive selection mechanisms have been used within the process. Data from a motion-based

Received 23 March 2015; revised 22 September 2015; accepted 8 October 2015.

six-degrees-of-freedom flight simulator were used to evaluate the performance in terms of percentage identification rates for a set of 2D non-self projections under several upset conditions.

NOMENCLATURE

Acronyms

AIS	artificial immune system
ANN	artificial neural networks
DOF	degrees-of-freedom
DR	detection rate
ERAU	Embry-Riddle Aeronautical University
FDIE	failure detection, identification, evaluation
FI	false identifications
HMS	hierarchical multi-self
IR	identification rate
L-R	left and right
NS	negative selection
PS	positive selection
SNSA	structured non-self approach
WVU	West Virginia University

Subscripts

N_{max}	maximum number of dimensions
N_f	number of features
N_{self}	total number of sub-selves
S_N	number of subsystems

1.0 INTRODUCTION

In recent years, the biological immune system of vertebrates has inspired new methodologies in computational intelligence to address real-world complex problems[1,2]. The artificial immune system (AIS) paradigm has shown promising potential in a variety of applications such as pattern recognition[3,4], robotics[5,6], computer security[7,8], data mining[9,10], adaptive controls[11-13]and anomaly detection[14,15]. Researchers from West Virginia University (WVU) and Embry-Riddle Aeronautical University (ERAU) have proposed an integrated framework for AIS-based solutions to the aircraft sub-system failure detection, identification, evaluation (FDIE) problem[16,17]. As part of this effort, a comprehensive set of methodologies for AIS design and optimisation have been developed and implemented[18-20]. As an integrated solution, the AIS paradigm has demonstrated the capability to address the high complexity and multi-dimensionality of aerospace systems with potential for aircraft health management and fault tolerance applications over extended areas of the flight envelope[20,21]. In addition, flight envelope reduction assessment using the AIS paradigm at post-failure conditions has also been investigated with promising results[22].

The AIS mechanism operates in a similar manner as does the biological immune system (according to the principle of self- and non-self discrimination) when it detects microbial and

https://doi.org/10.1017/aer.2016.15 Published online by Cambridge University Press

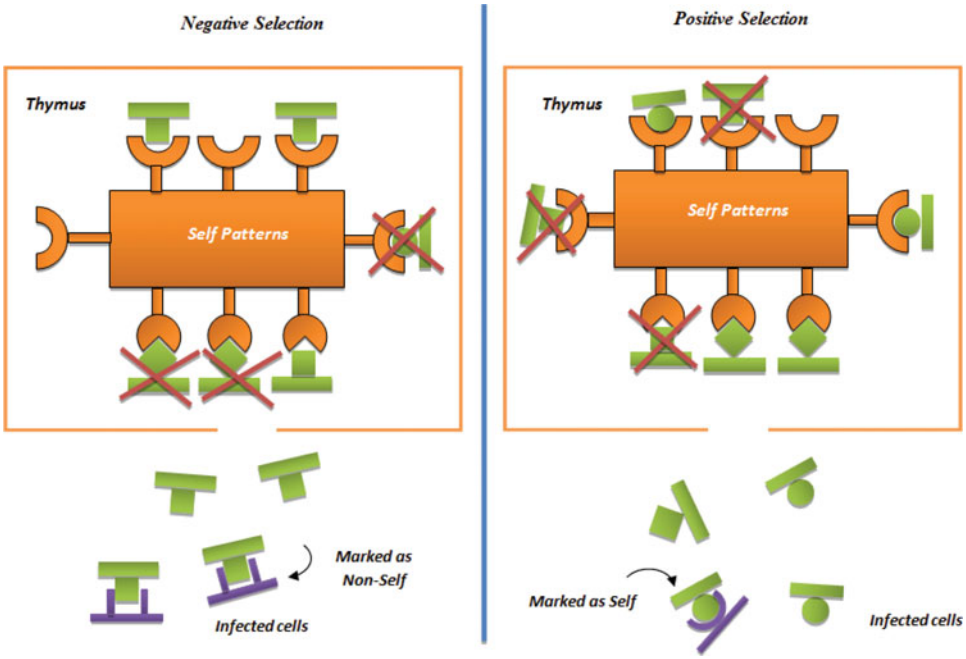

Figure 1. (Colour online) Negative and positive selection mechanisms.

non-microbial exogenous antigens while not reacting to the self cells[1,2,23]. T-cells are the component of the system with the most important role in this process. They are first generated through a pseudo-random genetic rearrangement mechanism, which ensures high variability of the new cells in terms of biological features (typically proteins or polysaccharides). A censoring process then takes place in the thymus resulting in the destruction of the T-cells that react against self proteins. Eventually, only those T-cells that do not bind to self proteins are allowed to leave the thymus to detect antigens and mark them for destruction. For obvious reasons, this process is referred to as negative selection (NS)[3]. Within the AIS paradigm, NS can be used to generate detectors by properly clustering the non-self hyperspace. Alternative mechanisms, based on positive selection (PS) have been explored for AIS as well. Through PS strategy, the detectors are generated to coincide with the self and the process is equivalent to clustering the self data. In this case, an abnormal situation is declared if the explored current configuration does not match any of the detectors. This is typically more computationally intensive as compared to the NS approach, in which the activation of a single negative anti-body is enough to declare the presence of abnormal situation. Using PS instead, it is necessary to test the complete set of positive anti-bodies before classifying a sample as abnormal. However, since the evaluation of a failure implies the diagnosis of its effects on the aircraft operational limits, the PS must be used to assess the distribution of the failure signature within the non-self by labelling the anti-bodies corresponding to different magnitudes of the failure. Figure 1 shows a representation of the NS and PS immune mechanisms.

Applying this paradigm to aircraft subsystem FDIE requires that a set of adequate features be defined. These features can include various sensor outputs, states estimates, statistical parameters or any other information expected to be relevant to the behaviour of the system and to be able to capture the signature of abnormal situations. Extensive experimental

https://doi.org/10.1017/aer.2016.15 Published online by Cambridge University Press

data are necessary to determine the self or the hyperspace of normal conditions. Adequate numerical representations of the self/non-self must be used and the data processed, such that they are manageable given the computational and storage limitations of the available hardware. In general, to make the AIS a practical aircraft health management technique, some specific aspects must be addressed: computational efficiency improvement of the algorithms, enhancement of the representation and development of unified architectures that can integrate several phases of the FDIE problem. Therefore, the development of failure detection, identification and evaluation schemes with high rates of success and comprehensive coverage, integrating all aircraft subsystems and operational modes, is a critical objective of this paper.

In previous efforts, the capability of the AIS paradigm to address the FDIE problem within a hierarchical multi-self (HMS) strategy has been demonstrated[19,25]. The HMS strategy relies on the premise that multiple non-self configurations or projections can be integrated in order to achieve good subsystem FDIE results[26]. In this paper, a structured non-self approach (SNSA) algorithm has been designed and implemented to increase the identification performance within the HMS strategy and extend its capabilities for classifying and quantifying the type and magnitude of different aircraft sub-systems' failures. Within this approach, sub-sets of anti-bodies or "identifiers" of specific non-selves are mapped against failures to categorise the dynamic fingerprint of the abnormal conditions throughout the entire flight envelope. Using a positive selection-type mechanism, the SNSA algorithm is able to determine which aircraft sub-system component is under an abnormal condition, the type of failure and the magnitude of the identified failure with a high identification rate (IR) and a low number of false identifications (FI).

The proposed identification mechanism consists of a dual phase multi-self approach in which pre-selected selves with acceptable detection rates are used for identification purposes. The first phase of the mechanism consists precisely of an off-line selection of selves that demonstrate to have good detection performance through experimentation. The second phase relies on a positive selection algorithm that determines specifically the failed sub-system, the failure type and the failure severity. It uses a logic strategy in which a failure is considered to be identified properly if the majority of identifiers agree on the identification outcome.

The paper is organised as follows. After a brief introduction, the AIS paradigm for aircraft sub-system abnormal condition identification is outlined in Section II. The process of generating the identifiers using positive selection algorithms and the identification algorithm is described in Section III. In Section IV, the simulation environment utilised is described. In Section V, the results of the identification algorithms are presented. The conclusions of this research effort are summarised in Section VI, followed by acknowledgments and a list of references.

2.0 AIS-BASED FDIE PROBLEM FORMULATION

The general identification problem must be defined and formulated in detail, including the sub-systems targeted, and the category and severity of the failure. Such a process, as shown in Fig. 2, can be performed in several phases to address the FDIE problem: within a first phase, an off-line process is performed to generate detectors based on a clear definition of the aircraft dynamic features. This process requires the availability of large amounts of measured data that must be pre-processed for self/non-self generation and structuring. For a comprehensive solution, acquiring and processing these data is considerably less difficult and

https://doi.org/10.1017/aer.2016.15 Published online by Cambridge University Press

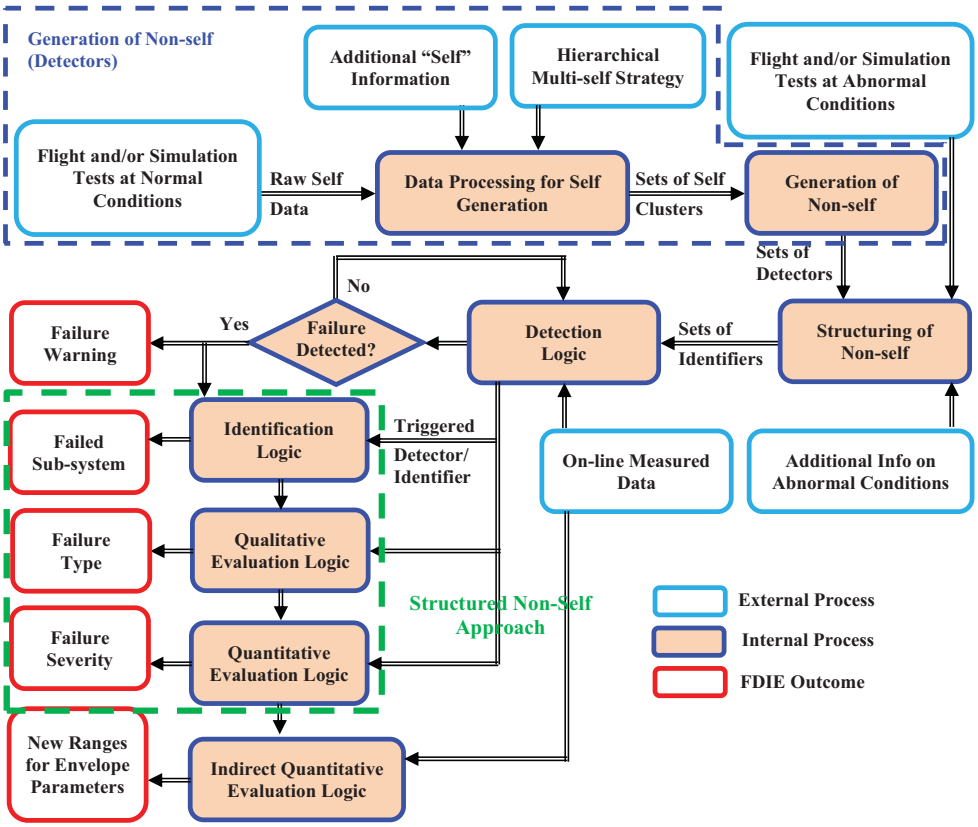

Figure 2. (Colour online) AIS general architecture.

expensive than developing extensive accurate models, as required by alternative approaches. The effectiveness of the abnormal condition feature selection is determined by the number of sub-selves used and the number of identifiers generated for each sub-system failure investigated. In a following phase, on-line abnormal condition detection, identification, and evaluation are performed. Sets of current values of the features measured in flight at a certain sampling rate are compared against the detectors, identifiers, and evaluators and the outcomes of the FDIE are generated. These outcomes could be transferred to the pilot, an on-board monitoring and recording system, and to automatic fault tolerant control laws. It is important to notice that the general architecture of the identification problem requires prior generation of the non-self with adequate resolution and knowledge of the abnormal condition characteristics. In previous efforts, this problem was addressed by considering the abnormal condition identification and evaluation as independent modules[16,17]. First, identification was defined as the determination of the subsystem affected by the abnormal condition. Then, evaluation was defined within a context of qualitative (type) and quantitative (severity or magnitude) assessment of the identified failure. In this paper, as shown in Fig. 2 with lower dotted lines, a preliminary integration of identification and evaluation phases into one unique scheme using a structured non-self approach is investigated. The performance is demonstrated

https://doi.org/10.1017/aer.2016.15 Published online by Cambridge University Press

Table 1
Feature list for aircraft AIS development

H = **altitude**	V = **aircraft ground speed**
d_e = longitudinal stick displacement	M = Mach number
d_a = lateral stick displacement	a_x = longitudinal acceleration
d_r = pedal displacement	a_Y = lateral acceleration
d_T = pilot throttle	a_z = vertical acceleration
p_{ref} = roll rate command	α = angle-of-attack
q_{ref} = pitch rate command	β = sideslip angle
r_{ref} = yaw rate command	ϕ = roll attitude angle
NN_p = estimates of roll acceleration error	θ =pitch attitude angle
NN_q = estimates of pitch acceleration error	ψ = yaw attitude angle
NN_r = estimates of yaw acceleration error	p = roll rate
$MQEE$ = main quadratic estimation error	q = pitch rate
$OQEE$ = output quadratic estimation error	r = yaw rate
$DQEE_p$ = decentralised quadratic roll rate estimation error	$\dot{p}$ = roll acceleration
$DQEE_q$ = decentralised quadratic pitch rate estimation error	$\dot{q}$ = pitch acceleration
$DQEE_r$ = decentralised quadratic yaw rate estimation error	$\dot{r}$ = yaw acceleration

through correct failure subsystem and magnitude classification which minimises the design process by using higher-resolution antibodies.

The identification structure presented in this paper relies on the selection of sub-selves previously tested for failure detection within an HMS scheme that features high flexibility and can extract the best characteristics of different features for FDIE purposes. The HMS strategy relies on the assumption that within a class of failures, differences in the dynamic fingerprint among failed elements may be captured by different features. Therefore, a specific set of parameters could favour the identification of some particular failures better than others[25].

Let us assume that four major aircraft sub-systems with their components must be considered, such as actuators, sensors, structural elements and propulsion. The set of actuators may include a left and right (L-R) stabilator, L-R aileron, L-R rudder and L-R throttle. The sensors considered may be the angular rate gyros, which are typically necessary for a multitude of automatic control systems. Let us assume that the targeted structural elements are a L-R wing, L-R horizontal tail and L-R vertical tail, and that the propulsion system consists of two engines. The total number of sub-systems S_N results to be $S_N = 8 + 3 + 6 + 2 = 19$.

The definition and analysis of the failures is important for the process of selecting and defining the features because they must capture the dynamic fingerprint of all failures. It should be noted that unknown failures can be detected as they are implicitly included in the non-self.

The feature variables are expected to completely define the targeted system and achieve the self/non-self-discrimination. An example set of features for aircraft AIS development is presented in Table 1. It includes system states, state derivatives and inputs, as well as derived and estimated parameters. Carefully designed derived parameters can often prove to be valuable AIS features. For example, the angular acceleration errors in Table 1 are artificial neural network estimates with excellent detection capabilities for a variety of abnormal

https://doi.org/10.1017/aer.2016.15 Published online by Cambridge University Press

conditions[28]. The quadratic estimation parameters are based on angular rates measurements and their neural network estimations[28] and have shown good detection capabilities for sensor failures[25].

With the set of features presented in Table 1, a 32-dimensional hyper-space must be handled to define the self and non-self. This can create significant computational problems. However, they can be mitigated or avoided altogether using the HMS strategy[19], which uses lower-order projections to build sub-selves instead of using one single higher-dimensional hyper-space and makes use of a specific hierarchy of feature relevance with respect to each type of failure. Therefore, projections of the hyper-space along relevant dimensions only may be enough to detect the respective failures. Within this research effort, an exhaustive set of 2D projections $N_{\max} = 2$ is used. The total number of sub-selves N_{self} that need to be built for a complete set with $N_f = 32$ features is: $N_{self} = C_N^{N_{\max}} = \frac{N_f!}{N_{\max}!(N_f - N_{\max})!} = \frac{32!}{2!30!} = 496$.

3.0 STRUCTURED NON-SELF APPROACH

The abnormal condition identification and evaluation processes investigated in this effort represent a novel and integrated approach for the problem of aircraft operation under sub-system failure within the HMS strategy. The approach is based on a structuring process of non-self-projections and intends to reduce the computational effort required and to facilitate the real-time application of the AIS approach without compromising the FDIE performance. As shown in Fig. 3, the proposed SNSA consists of a dual-phase algorithm where 2D self/non-self projections, previously generated using negative selection mechanism and tested in simulation under several abnormal conditions, are selected according to the ability to detect failures at a pre-defined detection rate (DR). Then, by using a positive selection-type mechanism, the resulting projections are processed to generate identifiers capable of differentiating similar dynamic prints among several abnormal conditions and declaring correct failure types and magnitudes. This process extends the capabilities of the identification phase by not only classifying but also providing a quantitative evaluation of the failure, as depicted in green in Fig. 2.

For example, within a first phase of the SNSA, a total of 496 self/non-self projections were generated based on the availability of 32 features to capture the dynamic print of abnormal conditions. After comparing these projections with all considered types of failures, the ones with a DR equal to or larger than 70% were selected as candidates. After this process, a total of 183 projections were considered to possess the ability to capture the dynamic print of several sub-system failures and, more importantly, facilitate the process of characterising the projections that perform better during the identification of specific failures. Table 2 presents a sample set of the 2D projections investigated within this phase.

The dynamic fingerprint of several failures may produce a very similar effect on the features of self/non-self projections. This characteristic presents a more complex problem in which incorrect identification may be produced if the identification problem is not defined appropriately. For example, let us assume that an identification algorithm, only consisting of *Self#3* (p_{ref}, NN_p), is tested for two sub-system failures (i.e. right wing structural failure and left aileron stuck failure). This particular pair of failures will produce an undesired roll rate that can be successfully perceived and detected by *Self#3*. The dynamic fingerprint produced by both abnormal conditions in the selected projection may look very similar, increasing the complexity of the identification problem. Now, let us assume that the same identification algorithm is augmented with *Self#30* (q_{ref}, NN_p) which can also capture the

https://doi.org/10.1017/aer.2016.15 Published online by Cambridge University Press

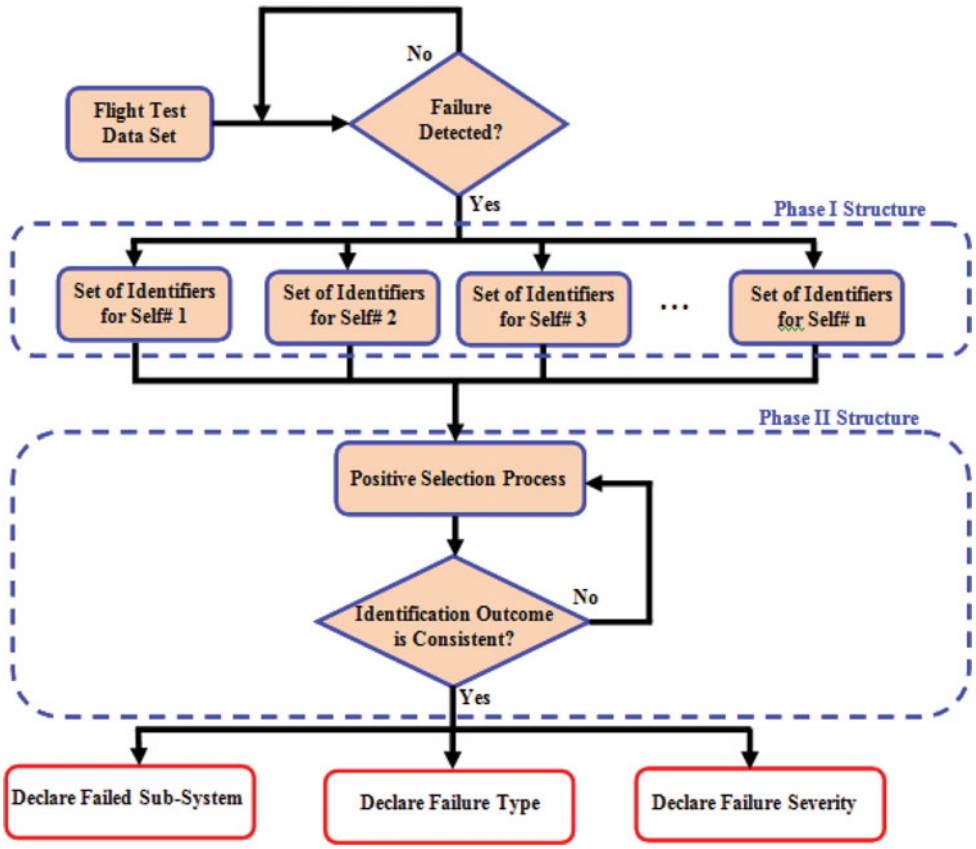

Figure 3. (Colour online) Structured non-self approach logic.

Table 2
Self/non-self projections

Self	Features	Self	Features
Self#3	p_{ref}, NN_p	Self#56	r_{ref}, NN_p
Self#4	p_{ref}, NN_q	Self#57	r_{ref}, NN_q
Self#7	$p_{ref}, OQEE$	Self#60	$r_{ref}, OQEE$
Self#8	$p_{ref}, DQEE_p$	Self#61	$r_{ref}, DQEE_p$
Self#9	$p_{ref}, DQEE_q$	Self#62	$r_{ref}, DQEE_q$
Self#30	q_{ref}, NN_p	Self#69	r_{ref}, r
Self#31	q_{ref}, NN_q	Self#82	NN_p, NN_q
Self#34	$q_{ref}, OQEE$	Self#83	NN_p, NN_r
Self#35	$q_{ref}, DQEE_p$	Self#84	$NN_p, MQEE$
Self#36	$q_{ref}, DQEE_q$	Self#85	$NN_p, OQEE$
Self#42	q_{ref}, q	Self#86	$NN_p, DQEE_p$
Self#52	q_{ref}, d_e	Self#87	$NN_p, DQEE_q$
Self#53	q_{ref}, d_r	Self#88	$NN_p, DQEE_r$

https://doi.org/10.1017/aer.2016.15 Published online by Cambridge University Press

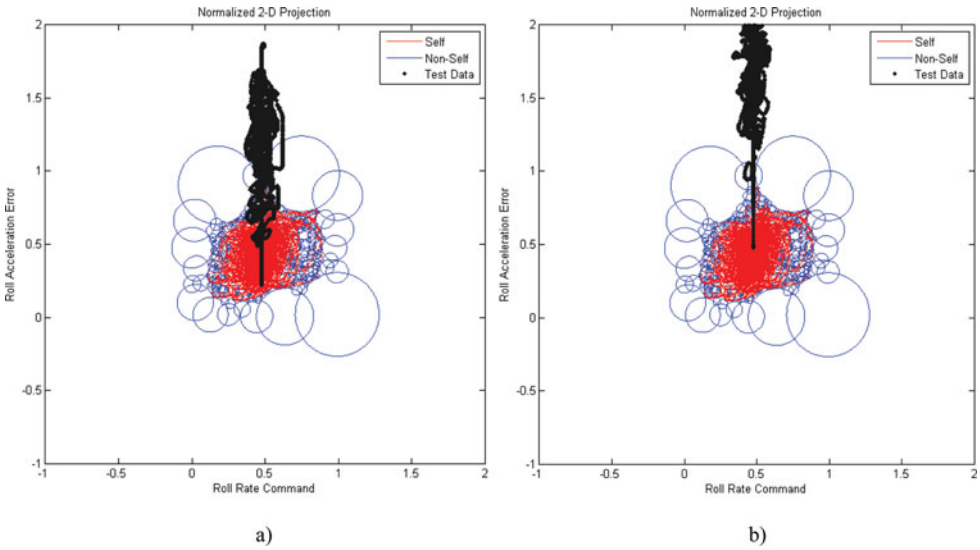

Figure 4. (Colour online) (a) Self#3 with left aileron failure, (b) Self#3 with right wing structural damage.

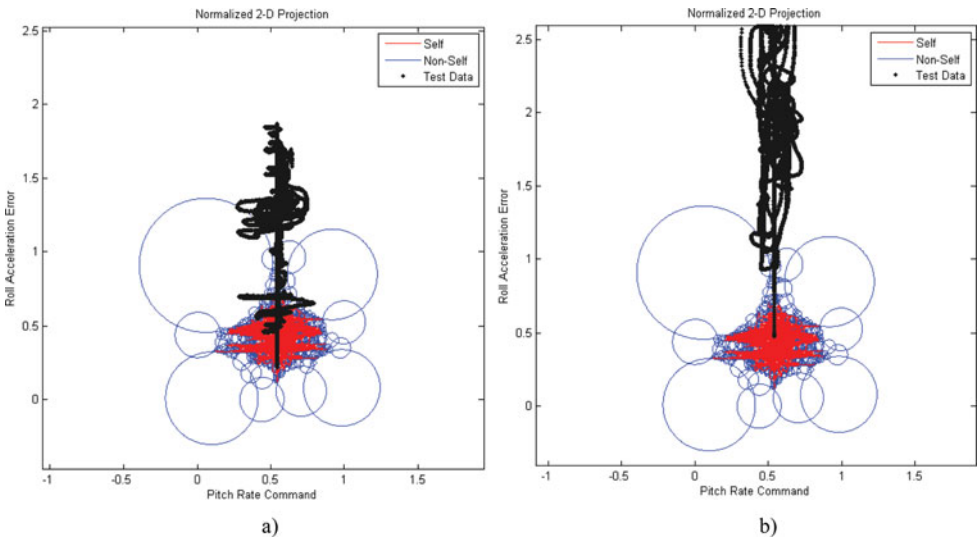

Figure 5. (Colour online) (a) Self#30 with left aileron failure, (b) Self#30 with right wing structural damage.

abnormal condition dynamic print of the mentioned failures. Due to the fact that *Self#30* also captures dynamic changes in pitch rate, it is possible to identify and distinguish between the two mentioned failures. Within a second phase of the SNSA, positive selection applied to the 183 self/non-self projections is performed in order to address the mentioned identification problem. Figures 4(a), 4(b), 5(a) and 5(b) present the similarity of the dynamic print of two different failures in a 2D projection.

The combined identification capabilities of the projections utilised within the two phases of the SNSA provides a more robust system capable of not only correctly identifying the

https://doi.org/10.1017/aer.2016.15 Published online by Cambridge University Press

Table 3
Investigated sub-system failures

Failure #	Failure	Failure #	Failure
1	Left aileron stuck at 2°	9	Left wing loss of 6%
2	Right aileron stuck at 2°	10	Right wing loss of 6%
3	Left aileron stuck at 8°	11	Left wing loss of 15%
4	Right aileron stuck at 8°	12	Right wing loss of 15%
5	Left stabilator stuck at 2°	13	Left engine out
6	Right stabilator stuck at 2°	14	Right engine out
7	Left stabilator stuck at 8°	15	Roll sensor bias of 5°/sec
8	Right stabilator stuck at 8°	16	Roll sensor bias of 10°/sec

detected failure but also providing information regarding the magnitude of the investigated failures. With the correct combination of projections with their corresponding identifiers, it is possible to discard incorrect failures and ultimately determine which abnormal condition is affecting the system.

3.1 Phase I: Non-self 2D projections selection

The first phase of the SNSA is the result of the failure detection testing within the HMS strategy. As mentioned previously, 496 2D self/non-self projections were generated for failure detection algorithm experimentation. Then, they were tested against over 16 different failures including several sub-systems under different failure magnitudes. Extensive experimentation was required in order to determine which projections could substantially detect a failure with good detection rates and minimum false alarms within a negative selection approach. It was determined that a total of 183 projections were capable to fulfil the objectives of a DR equal to or higher than 70%. This process is referred to as the Phase I Non-Self Structuring. The selected projections as potential candidates for identification included sensor outputs, state estimates and statistical parameters, among other features. The set of abnormal conditions involved sensor failures, structural damage on the wings, engine failures and control surface failures. Table 3, shown below, presents a list of the failures investigated in this research effort.

Several failures presented similar dynamic fingerprints on several 2D projections, which subsequently led to the selection of several projections with the ability to detect multiple failures. On the other hand, certain failures that are difficult to detect, such as rudder failure, only resulted in the activation of a few projections. The selection logic behind Phase I of the algorithm resulted in the reduction of the initial number of projections down to a significantly smaller set, thus reducing the complexity and the hardware requirements for algorithm implementation. Table 4 presents a sample of the projections that are considered to be adequate for abnormal condition identification based on the detection performance equal to or higher than 70%. In this table, the results are presented based on the detection capability of the sample set of projections for five sample types of failures at different magnitudes. This analysis was performed on the 496 original projections under 16 failures, varying in sub-system categories, failures types and magnitudes. Various projections present the ability to capture the dynamic fingerprint of several abnormal conditions, while others can only capture the dynamics of a small set or even a single abnormal condition. For example, *Self#3* demonstrated its ability to capture the dynamic fingerprint of a locked left aileron, a right

https://doi.org/10.1017/aer.2016.15 Published online by Cambridge University Press

Table 4
Detection performance of a sample set of projections

Self/ Failure	Left Aileron Stuck 2°	Left Aileron Stuck 8°	Right Wing 6% Struct. Damage	Right Wing 15% Struct. Damage	Left Stab. Stuck 2°	Left Stab. Stuck 8°	Right Engine Out	Roll Sensor 5°/s Bias	Roll Sensor 10°/s Bias
Self#3	82.02	99.95	99.84	99.98	99.38	99.96	10.51	1.90	3.42
Self#4	1.45	1.82	3.87	13.76	30.73	99.85	1.42	3.02	4.08
Self#30	83.49	99.95	99.83	99.98	99.29	99.96	10.57	2.82	30.02
Self#31	0.85	3.26	1.94	0.87	28.99	99.82	0.52	0.37	60.68
Self#52	0.99	2.64	0.76	17.53	1.75	1.56	1.10	0.96	71.52
Self#56	86.85	99.93	99.94	99.94	99.48	99.88	12.94	5.43	0.59
Self#82	92.33	99.96	99.96	99.98	99.73	99.97	21.32	7.67	15.01
Self#83	88.06	99.96	99.93	99.98	99.62	99.97	14.13	5.81	0.74
Self#84	86.23	99.96	99.94	100	99.52	99.98	12.05	2.81	0.30
Self#85	88.76	99.97	99.91	99.98	99.45	99.96	12.80	40.66	37.42
Self#100	86.92	99.51	99.45	99.48	99.08	99.25	15.20	3.09	0.46
Self#142	0.06	1.60	29.35	49.08	17.11	56.08	72.42	0.35	0.99
Self#233	5.51	8.40	7.47	10.26	8.04	7.02	5.49	68.53	92.07
Self#259	13.44	18.26	54.05	45.79	32.52	77.33	72.54	7.30	9.41
Self#350	15.39	17.70	33.10	40.93	22.74	60.70	72.47	30.82	22.27
Self#351	26.07	24.21	50.30	46.33	32.38	67.13	71.49	7.38	14.23
Self#433	1.39	3.43	1.44	14.07	2.77	6.76	2.33	3.89	77.7

Table 5
Total number of projections activated per failure

Actuator						Engine		Structural	
Aileron Stuck (8°)		Stabilator Stuck (8°)		Rudder Stuck (8°)		Engine Out		Wing Damage (15%)	
Left	Right	Left	Right	Left	Right	Left	Right	Left	Right
31	31	72	62	9	11	31	4	31	31

wing with structural damage and a left stabilator locked failure. On the other hand, *Self#4* only demonstrates the ability to capture the dynamic fingerprint of a "left stabilator locked"-type of failure. In addition, from Table 4, it is possible to highlight that specific projections would have the capability to detect a specific failure at different severities.

Within this analysis, it was possible to isolate the projections that can be used for identification purposes. From the Phase I non-self structure analysis, it was possible to determine which specific projections correspond to every specific failure investigated. Furthermore, it is also possible to determine how many projections capture the dynamic fingerprint of any given abnormal condition at different magnitudes. Table 5 presents an

https://doi.org/10.1017/aer.2016.15 Published online by Cambridge University Press

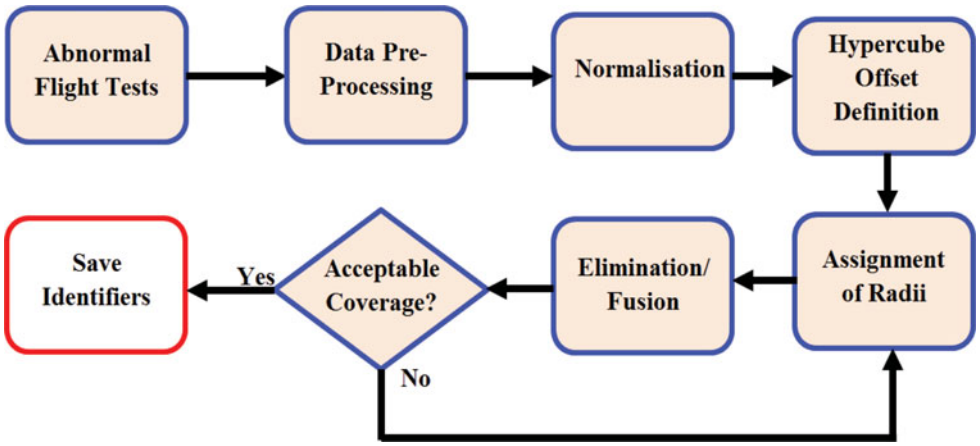

Figure 6. (Colour online) Identifier generation logic.

example of the number of projections from the total 183 selected that have the potential ability to be used for identification purposes.

As a result of the Phase I non-self structuring, the total number of projections needed to perform the FDIE algorithm is considerably reduced. This outcome allows a more efficient design of the mapped-based positive selection algorithm utilised in the second phase of the SNSA.

3.1 Phase II: Positive selection algorithm

Phase II of SNSA includes a positive selection-type process where flight failure test data are used to generate higher-resolution non-self detectors that are labelled depending on the characteristics of the failure, and thus, converted into identifiers. Resulting projections from Phase I are processed in order to generate identifiers capable of differentiating similar dynamic prints among several abnormal conditions and declaring correct failure types and magnitudes. In order to obtain correct identification results, the identification logic must be carefully formulated and the generation and selection of identifiers must be adequate. Sub-sets of antibodies or identifiers must be generated with sufficient resolution to avoid incorrect outputs. The generation of identifiers consists of a multi-step process where their radii are assigned based on their distance to self and not based on coverage of the non-self optimisation criteria, as was the case for previous detector generation. Figure 6 presents the logic for the generation of identifiers.

Abnormal Flight Tests: Several flight tests at different abnormal conditions throughout the entire flight envelope are performed. Previously selected features corresponding to the self/non-self definition as shown in Table 1 are recorded for future processing and identifier definition. Section IV provides more details on the flight testing environment and conditions.

Normalisation: The sets of raw data received from the flight tests' recorded values are normalised between 0 and 1. The normalisation factor of each projection is determined by the range of the flight data plus a percent margin. The normalisation factor is the same one used for the self/non-self projections during the antibodies generation[26]. Therefore, the

https://doi.org/10.1017/aer.2016.15 Published online by Cambridge University Press

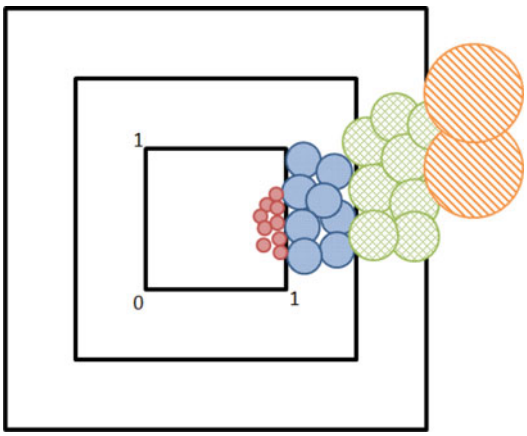

Figure 7. (Colour online) Radii variation with respect to distance from the self.

normalised data points of failure data correspond to the correct hypercube projection of each specific feature combination.

Offset Hypercubes: The unit hypercube determined during the normalisation process delimits the hyperspace of the nominal condition flight tests. High-magnitude failures may contain data points that lie far away from the unit hypercube of the self/non-self projection. Therefore, outward concentric hypercubes are defined in order to determine the distance of the abnormal condition point from the self, which subsequently allows the algorithm to determine the magnitude of the corresponding failure (see Fig. 7).

Radii Assignment: The radius of any identifier is pre-determined and it is assigned depending on the location of its centre with respect to the offset hypercubes. Since 2D projections are used, the radii that correspond to identifiers at each area are previously established based on direct observation of few selves against abnormal condition signatures. The radius of an identifier increases as the position of its centre lies within an outward hypercube. In other words, the radii of all identifiers increase as their distance to the self increases. The increase of the radii of the identifiers is due to the fact that higher-magnitude failures are expected to present a dynamic fingerprint with greater dispersion of data points.

Identifiers Elimination/Fusion: The amount of initial identifiers depends on the number of data points obtained from the flight tests. This may yield a very large number of identifiers that will require excessive computer processing capabilities. A simple elimination algorithm is implemented in order to reduce the number of identifiers. Identifiers that lay inside the radius of another identifier, plus a tolerance, are eliminated. Finally, a fusion process is performed that consists of a set union accompanied by overlapping elimination. After this step is concluded, the final number of identifiers is reduced considerably.

The identifiers generated during Phase I and II are then loaded into an identification function and organised in a single array such that the index of each identifier corresponds to a failure type and magnitude. The arrangement of the identifiers is inspired by a mapping-based algorithm which simplifies the selection scheme. The positive selection process is performed simultaneously by all the projections included in the identification algorithm. The outputs of all projections are compared to each other and the most frequent value is determined. If a

https://doi.org/10.1017/aer.2016.15 Published online by Cambridge University Press

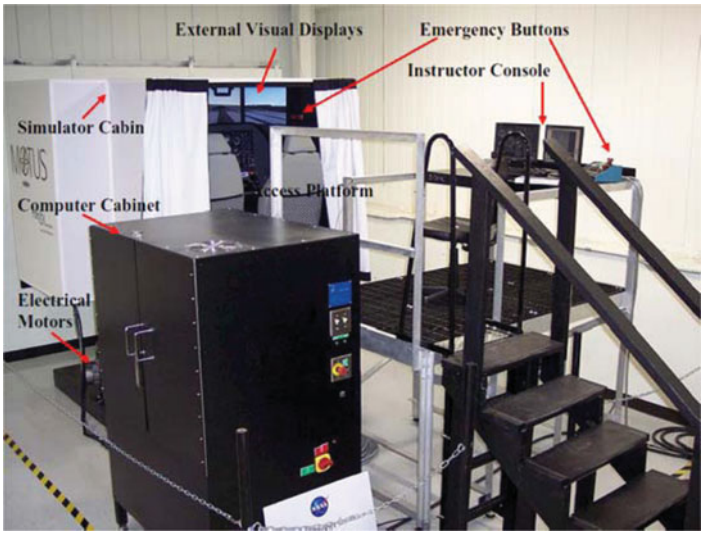

Figure 8. (Colour online) The WVU 6-DOF motion-based flight simulator.

specific failure index is present throughout the majority of the projections' outputs, its value is selected and a proper identification is declared.

The approach investigated in this paper covers not only a general identification logic, but also a quantitative evaluation logic integrated into a single, less complex algorithm. This integration intends to reduce the computational process for the real-time implementation of the solution to the FDIE problem. The mapping-based positive selection logic proposed here targets a multi-dimensional problem by means of a simpler but effective logic that can result in a more efficient real-time algorithm.

4.0 THE SIMULATION ENVIRONMENT

Experimental data was collected from the WVU 6-DOF Flight Simulator system shown in Fig. 8. The simulator consists of a Motus 600 motion platform driven by electrical induction motors to provide adequate 6-DOF translational and rotational motion cues. The motion platform was inter-faced with an external computer on which an aircraft model can run within the Matlab/Simulink environment to drive the entire simulator system. The aircraft model used in this work is a customised research supersonic fighter aircraft[19]. This aircraft also includes model reference adaptive control laws based on non-linear dynamic inversion and artificial neural network (ANN) augmentation, which also produces estimates of the aircraft angular rates and angular acceleration errors.

The AIS self/non-selves were generated from data collected for different flight scenarios under normal conditions over a wide range of the flight envelope. Nine reference points for various altitude/Mach number combinations were used in designing these flight scenarios as shown in Fig. 9. All flight tests start at steady state flight conditions at point 1 and continue to cover the nine points as described by the arrows. For example, for a flight scenario 1-2-3, the aircraft climbs from point 1 to point 2 with constant speed, accelerates from point 2 to point 3 with constant altitude, decelerates from point 3 to point 2 with constant altitude, and descends from point 2 to point 1 with constant speed. A total of eight such tests are necessary to cover

https://doi.org/10.1017/aer.2016.15 Published online by Cambridge University Press

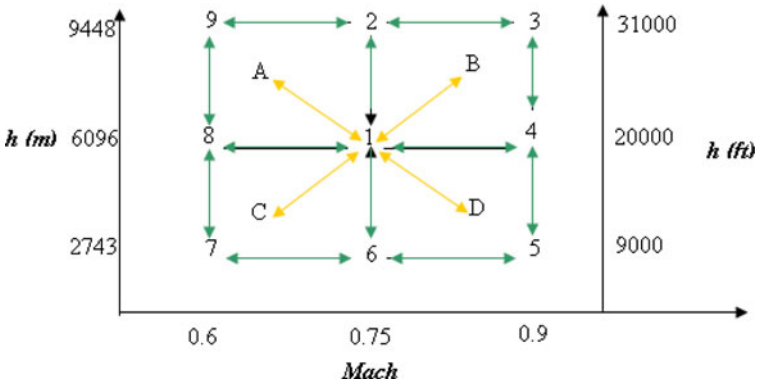

Figure 9. (Colour online) Testing flight envelope.

Table 6
The aircraft sub-systems and their failure types

Sub-system Category	Sub-system	Description
Actuator	Left/Right Stabilator Left/Right Aileron Left/Right Rudder	Blockage of any control surface at non-trim position
Sensor	Roll Gyro Pitch Gyro Yaw Gyro	LSB: large step bias LFDB: large fast drifting bias
Structure	Left/Right Wing	Missing part of the wing with and without affecting the "efficiency" of the aileron control surface.
Propulsion	Left/Right Engine	Reduced effectiveness /Loss of power in one of the engines

the testing flight envelope. Additional intermediate points (A, B, C and D in Fig. 9) were used for validation. Note that all flight scenarios include mild to moderate manoeuvres and that the data acquisition rate from the simulator is 50 Hz.

Table 6 summarises the aircraft sub-systems and the failure types considered for the purpose of this paper. A total of 13 sub-systems were modelled to support the development and testing of the AIS-based FDIE scheme. Failure test data were collected from the simulator using the same testing flight envelope as that of Fig. 9. Only one failure at a time was considered to capture/isolate the dynamic fingerprint of each type of failure and generate antibodies appropriately.

5.0 RESULTS

The identifier generation algorithm proposed in this research effort was implemented for nine different failures considered to be high magnitude using the 183 selected projections.

https://doi.org/10.1017/aer.2016.15 Published online by Cambridge University Press

Table 7
Projections used for identification

Self#	Features	Self#	Features	Self#	Features	Self#	Features
3	p_{ref} NN_p	57	r_{ref} NN_q	110	NN_q $DQEEp$	121	NN_q φ
4	p_{ref} NN_q	60	r_{ref} $OQEE$	111	NN_q $DQEEq$	123	NN_q ax
7	p_{ref} $OQEE$	82	NN_p NN_q	113	NN_q υ	124	NN_q ay
9	p_{ref} $DQEEq$	83	NN_p NN_r	114	NN_q α	125	NN_q az
31	q_{ref} NN_q	84	NN_p $MQEE$	115	NN_q β	126	NN_q d_a
34	q_{ref} $OQEE$	86	NN_p $DQEEp$	116	NN_q p	127	NN_q d_e
35	q_{ref} $DQEEp$	87	NN_p $DQEEq$	117	NN_q q	128	NN_q d_r
42	q_{ref} q	88	NN_p $DQEEr$	118	NN_q r	129	NN_q d_T
56	r_{ref} NN_p	107	NN_q NN_r	120	NN_q θ	130	NN_q M

Based on the assumption that lower-magnitude failures of the same type of failure generate similar dynamic fingerprints with a closer proximity to the self, the set of identifiers were subdivided into two groups. The first set corresponds to high magnitude and the second set to low-magnitude failures (i.e. closer to the self). This approach increases the total amount of failures that can be identified to 18 instead of the original 9. A total of 1647 different cases for identifier generation were implemented in order to cover all the possible failure outputs investigated.

Each set of identifiers generated per failure contains on average 36 identifiers. Considering that every set of identifiers for all failures is integrated in each projection, an approximate total of 324 identifiers per projection are used for the identification positive selection process.

After an initial analysis, the algorithm was optimised and it was determined that out of the 183 projections, a total of 93 projections were enough to correctly identify the investigated failures. The reduction of the total number of projections required for identification will reduce computational complexity of the algorithm considerably.Table 7 presents a sample set of projections used for failure identification.

Further analysis was carried out to reduce the number of projections required to produce desirable identification outputs. In some cases, the use of a single projection was enough to obtain favourable identification rates. On the other hand, other failures require more projections in order to obtain desirable identification results and also to reduce misidentification rates. Table 8 presents the number of projections required for a correct failure identification output.

The identification algorithm was tested under 16 different failures (refer to Table 3). Table 9, shown below, presents the results for identification rate analysis. It includes the false identification percent for other types of failures. It should be noted that, in some cases, the dynamic fingerprint of a failure fell outside the identifiers. For these particular cases the identification algorithm output a 0% identification rate. For simplicity, a "no identified failure" column was not included in Table 9. It should be noted that Table 9 presents the identification results in a horizontal fashion. For example, failure #1 is output correctly 99.7% of the time but presents confusion with failures 3, 4 and 14 for 0.1% of the time, respectively.

https://doi.org/10.1017/aer.2016.15 Published online by Cambridge University Press

Table 8
Total number of projections used for identification

Failure #	Failure	Projections Used	Failure #	Failure	Projections Used
1	Left aileron stuck at 2°	14	9	Left wing loss of 6%	2
2	Right aileron stuck at 2°	7	10	Right wing oss of 6%	1
3	Left aileron stuck at 8°	8	11	Left wing loss of 15%	1
4	Right aileron stuck at 8°	8	12	Right wing loss of 15%	2
5	Left stabilator stuck at 2°	18	13	Left engine out	1
6	Right stabilator stuck at 2°	2	14	Right engine out	18
7	Left stabilator stuck at 8°	9	15	Roll sensor bias of 5°/sec	1
8	Right stabilator stuck at 8°	31	16	Roll sensor bias of 10°/sec	7

6.0 CONCLUSIONS

A novel, more compact SNSA algorithm for aircraft sub-system failure identification and evaluation has been developed and tested for several abnormal conditions. The algorithms for generation of identifiers through positive selection and the structuring of the non-self have been described and implemented successfully. This novel two-phase SNSA algorithm has been developed within a fault tolerance architecture to address aircraft sub-system failure detection, identification and evaluation FDIE problems. The approach relies on a new refined process to extend and enhance the architecture capabilities. The first phase corresponds to non-self-structuring via negative selection, in which 2D, self/non-self-projections are selected according to the ability to detect failures at a pre-defined detection rate. A second phase uses positive selection to generate specific sets of detectors capable of differentiating similar dynamic prints among several abnormal conditions and declaring correct failure types and magnitudes.

The identification performance was obtained through a set of 93 2D projections within an HMS strategy and, as shown from the results, achieved excellent performance in terms of identification rate for 16 types of failures. The results demonstrate that the proposed methodology is able to reduce the total number of projections required to successfully identify failed subsystems without compromising the FDIE performance. The total number of projections was reduced from 496 to 93. This projection reduction implies less overall complexity and computational time required to execute an effective algorithm, making this approach feasible for real-time execution. The capability of the SNSA for failure identification and evaluation using a small number of low-dimensional projections was confirmed.

https://doi.org/10.1017/aer.2016.15 Published online by Cambridge University Press

https://doi.org/10.1017/aer.2016.15 Published online by Cambridge University Press

Table 9
Identification results for 16 different failures

		Identified Failure #															
		1	**2**	**3**	**4**	**5**	**6**	**7**	**8**	**9**	**10**	**11**	**12**	**13**	**14**	**15**	**16**
Failure #	1	**99.7**	0	0.1	0.1	0	0	0	0	0	0	0	0	0	0.1	0	0
	2	9.9	**87.3**	0	0	0	0	0	0	0	0	0	0	0	2.8	0	0
	3	0.4	0	**95.6**	0.6	0	0	0	0	0	0	0	0	0	3.4	0	0
	4	0	0	0.1	**97.2**	0	0	0	0	0	0	0	0	0.3	2.4	0	0
	5	0.5	1.7	1.5	0	**92.5**	1.5	1.1	0	0	0	0	0	0	0	1.2	0
	6	9.9	0	1.2	0	0	**86.8**	0	2.1	0	0	0	0	0	0	0	0
	7	0.2	1	0	0	0	0	**96.1**	1.5	0	0	0	1.2	0	0	0	0
	8	0.5	0	0	0	0	0	4.8	**93.8**	0.9	0	0	0	0	0	0	0
	9	1.2	2	0.2	0	0	0.1	0	0.9	**95.6**	0	0	0	0	0	0	0
	10	0	0	2.1	0	0	0	0	0	1.1	**94.5**	0	0	0	1.1	0	1.2
	11	0	0	0	0	0	0	0	0.1	7.6	0.1	**92.2**	0	0	0	0	0
	12	0	0	0	0	0	0	1.1	0	0	1.1	0	**97.5**	0.3	0	0	0
	13	0	0	0	0	0	0	0	0	0	0	0	0	**92.6**	7.4	0	0
	14	0	0	0	0	0	0	0	0	0	0	0	0	0.1	**99.9**	0	0
	15	0	0	0	0	0	0.3	0	0.2	0.3	0	0.2	0	2.1	1.3	**95.6**	0
	16	0	0	0	0.3	0	0	0	0	0	0	2.7	0	0	2.1	0	**94.9**

The data used for processing, design and validation of the proposed algorithms are based on information collected from human piloted tests performed on a high-fidelity 6-DOF motion-based simulator. In this sense, the results achieved and presented in this paper represent promising advancement towards real implementation of these AIS-based algorithms for FDIE on aerospace systems.

ACKNOWLEDGEMENT

This research effort has been supported by DARPA Tactical Technology Office under contract number HR0011-13-C-0024. The views expressed are those of the authors and do not reflect the official policy or position of the Department of Defense or the US Government.

REFERENCES

1. DASGUPTA, D. (Ed). *Artificial Immune Systems and Their Applications*, 1999, Springer-Verlag, New York, New York, US.
2. DASGUPTA, D. and NINO, L.F. *Immunological Computation – Theory and Applications*, 2009, CRC Press, Auerbach Publications, Taylor & Francis Group, Boca Raton, Florida, US.
3. DASGUPTA, D. and NINO, F. Comparison of negative and positive selection algorithms in novel pattern detection, Proceedings of the IEEE International Conference on Systems, Man and Cybernetics, 2000, Nashville, Tennessee, US, pp 125-130.
4. DE CASTRO, L. and TIMMIS, J. Artificial immune systems: A novel paradigm to pattern recognition, *Artificial Neural Networks in Pattern Recognition*, in CORCHADO, J. M., ALONSO, L., FYFE, C. (Eds), SOCO-2002, 2002, University of Paisley, UK, pp 67-84.
5. LAU, H.Y.K. and KO, A. An immune robotic system for humanitarian search and rescue, Proceedings of ICARIS 2007, Lecture Notes in Computer Science, 2007, Springer, Santos.
6. LEE, J., ROH, M., LEE, J. and LEE, D. Clonal selection algorithms for 6-DOF PID control of autonomous underwater vehicles, Proceedings of ICARIS 2007, Lecture Notes in Computer Science, 2007, Vol 4628, Springer-Verlag Berlin Heidelberg, pp 182-190.
7. HOFMEYR, S.A., SOMAYAJI, A. and FORREST, S. Intrusion detection using sequences of system calls, *J Computer Security*, 1998, **6**, pp 151-180.
8. TWYCROSS, J. and AICKELIN, U. Libtissue-implementing innate immunity, Proceedings of IEEE World Congress on Computational Intelligence, 2006, Vancouver, Canada.
9. SERAPIAO, A.B.S., RICARDO, J., MENDES, P. and MIURA, K. Artificial immune systems for classification of petroleum well drilling operations, Proceedings of the 6th International Conference on Artificial Immune Systems (ICARIS), 2007, Lecture Notes in Computer Science, 2007, Vol 4628, Springer-Verlag Berlin Heidelberg, pp 47-58.
10. TIMMIS, J. and KNIGHT, T. Artificial immune systems: Using the immune system as inspiration for data mining, in ABBASS, H.A., SARKER, R.A., NEWTON, C.S. (Eds), *Data Mining: A Heuristic Approach*, 2001, Idea Group Publishing, Hershey, Pennsylvania, US, pp 209-230.
11. KARR, C., NISHITA, K. and GRAHAM, K. Adaptive aircraft flight control simulation based on an artificial immune system, *Applied Intelligence*, 2005, **23**, (3), pp 295-308.
12. MONCAYO, H., PERHINSCHI, M.G., WILBURN, B., WILBURN, J. and KARAS, O. UAV adaptive control laws using non-linear dynamic inversion augmented with an immunity-based mechanism, Proceedings of the AIAA Guidance, Navigation, and Control Conference, 2012, Minneapolis, Minnesota, US.
13. TAKAHASHI, K. and YAMADA, T. Application of an immune feedback mechanism to control systems, *The Japan Soc Mechanical Engineers, JSME Int J, Series C*, 1998, **41**, (2), pp 184-191.
14. GONZALEZ, F., DASGUPTA, D. and KOZMA, R. Combining negative selection and classification techniques for anomaly detection, Proceedings of the 2002 Congress on Evolutionary Computation CEC2002, IEEE Press, 2002, Honolulu, Hawaii, US, pp 705-710.
15. GUZELLA, T.S., MOTA-SANTOS, T.A. and CAMINHAS, W.M. A novel immune inspired approach to fault detection, Proceedings of ICARIS 2007, Lecture Notes in Computer Science, 2007, Vol 4628, Springer-Verlag Berlin Heidelberg, pp 107-118.

https://doi.org/10.1017/aer.2016.15 Published online by Cambridge University Press

16. PERHINSCHI, M.G., MONCAYO, H. and DAVIS, J. Integrated framework for artificial immunity-based aircraft failure detection, identification, and evaluation, *AIAA J Airc*, 2010, **47**, (6), pp 1847-1859.
17. PERHINSCHI, M.G., MONCAYO, H. and AL AZZAWI, D. Integrated immunity-based framework for aircraft abnormal conditions management, *AIAA J Airc*, 2014, **51**, (6), pp 1726-1739, doi: 10.2514/1.C032381.
18. DAVIS, J., PERHINSCHI, M.G. and MONCAYO, H. Evolutionary algorithm for artificial immune system-based failure detector generation and optimization, *AIAA J Guidance, Control, and Dynamics*, 2010, **33**, (2), pp 302-320.
19. MONCAYO, H., PERHINSCHI, M.G. and DAVIS, J. Aircraft failure detection and identification using an immunological hierarchical multi-self strategy, *AIAA J Guidance, Control, and Dynamics*, 2010, **33**, (4), pp 1105-1114.
20. MONCAYO, H., PERHINSCHI, M.G. and DAVIS, J. Artificial immune system – based aircraft failure detection and identification over an extended flight envelope, *Aeronaut J*, 2011, **115**, (1163), pp 43-55.
21. MONCAYO, H., PERHINSCHI, M.G. and DAVIS, J. Simulation environment for the development and testing of immunity-based aircraft failure detection schemes, Proceedings of the AIAA Modeling and Simulation Technologies Conference, 2011, Portland, Oregon, US.
22. MONCAYO, H., PERHINSCHI, M.G. and DAVIS, J. Artificial-immune-system-based aircraft failure evaluation over extended flight envelope, *AIAA J Guidance, Control, and Dynamics*, 2011, **34**, (4), pp 989-1001.
23. DASGUPTA, D., KRISHNA KUMAR, K., WONG, D. and BERRY, M. Negative selection algorithm for aircraft fault detection, Proceedings of ICARIS 2004, LNCS3239, 2004, pp 1-13.
24. JANEWAY, C.A., TRAVERS, P., WALPORT, M. and SHLOMCHIK, M.J. *Immunobiology: The Immune System in Health and Disease*, 6th ed, 2005, Garland Science, New York, New York, US.
25. MONCAYO, H. and PERHINSCHI, M. *Aircraft Fault Tolerance: A Biologically Inspired Immune Framework for Sub-System Failures*, 2011, VDM Verlag Dr. Muller GmbH & Co. KG, VDM Publishing House Ltd., Saarbruecken, Germany.
26. PERHINSCHI, M.G., MONCAYO, H., AL AZZAWI, D. and MOGUEL, I. Generation of artificial immune system antibodies using raw data and cluster set union, *Int J Immune Computation*, 2014, **2**, (1), pp 1-15.
27. PERHINSCHI, M.G., MONCAYO, H., WILBURN, B., BARTLETT, A., DAVIS, J. and KARAS, O. Neurally-augmented immunity- based detection and identification of aircraft sub-system failures, *The Aeronaut J*, 2014, **118**, (1205), pp 775-796.
28. PERHINSCHI, M.G., NAPOLITANO, M.R., CAMPA, G., FRAVOLINI, M.L. and SEANOR, B. Integration of sensor and actuator failure detection, identification, and accommodation schemes within fault tolerant control laws, *Control and Intelligent Systems*, 2007, **35**, (4), pp 309-318

https://doi.org/10.1017/aer.2016.15 Published online by Cambridge University Press